Continuous Hicksian Trade Cycle Model with Consumption and Investment Time Delays*

Akio Matsumoto
Department of Systems and Industrial Engineering
University of Arizona,
Tucson, Arizona, 85721-0020, USA
akiom@email.arizona.edu
and
Department of Economics
Chuo University,
742-1, Higashinakano
Hachioji, Tokyo, 192-0393 JPN
akiom@tamacc.chuo-u.ac.jp

Ferenc Szidarovszky
Department of Systems and Industrial Engineering
University of Arizona,
Tucson, Arizona, 85721-0020, USA

Abstract

The main purpose of this paper is to consider effects caused by time delays on stability of continuous models when the dynamic system is piecewise differentiable. To this end, we construct a continuous version of the discrete Hickisan trade cycle model and introduce continuously distributed time delays. It is demonstrated that time delays stabilize an otherwise unstable system, and a piecewisely-connected limit cycle is generated around an unstable stationary state.

keywords: hybrid dynamical system, continuously distributed time lag, piecewisely-connected limit cycle, nonlinear multiplier-acclerator model

*The earlier verion of the paper was presented at the conference on *Transdisplineary Perspectives on Economic Complexity* held on May 17, 2008 at James Madision University, VA, USA. The authors wish to give special thanks to Duncan Foley and Laura Gardini for their helpful comments.

1 Introduction

It has been a well-known fact of advanced market economies that national income exhibits persistent and irregular fluctuations. Although linear models with exogenous shocks may be aperiodic, it has been a main interest in studying macro dynamics to detect endogenous sources of such dynamic behavior. If we look at the classic literature of the 1940's and 1950's, we find that Kaldor (1940), Hicks (1950) and Goodwin (1951) constructed nonlinear macro dynamic models and gave rise to persistent endogenously-driven cyclic fluctuations. Since newly-developing nonlinear theory involving chaos is introduced into economics in the middle 1970's, these "classic" nonlinear models in discrete-time and continuous-time has been reconsidered with these new tools.

The Kaldor model, which originally has a continuous time scale, "has served as the prototype model for nonlinear dynamic system in economics,"(Lorenz (1993), p.43) and has been extended in many directions. Chang and Smyth (1971) applies the Pointcare-Bendixon theorem to prove the existence of a Kaldorian limit cycle. Lorenz (1993) deals with a continuous Kaldor model to obtain a Hopf bifurcation to a limit cycle. Dana and Malgrange (1984) shows that a discrete Kaldor model can be chaotic if the nonlinearity of investment function becomes stronger. Concerning the Goodwin model, which is also originally continuous, Lorenz (1987) replaces autonomous outlays with a time-dependent outlay function and shows that the modified Goodwin model generates chaotic motion. Matsumoto (2008) shows that multiple limit cycles may coexist when a stationary state of the continuous Goodwin model is locally stable. Sushko, Puu and Gardini (2006) consider the discrete time Goodwin model and a number of bifurcation sequences for attractors and their basins are studied. The Hicks model, which was originally constructed in discrete time, is also re-examined. Hommes (1993, 1995) shows that the discrete Hicks model yields chaos when consumption and/or investment is distributed over several periods. Later, Gardini, Puu and Sushko (2006) complement Hommes' work and present a two-dimensional bifurcation diagram in which a birth of attracting cycles with different periods is shown. Puu (2007) includes the stock of capital in the Hicks model that generates chaos. These studies indicate that nonlinear macro model of a dynamic economy may explain various complex dynamic behavior of economic variables including national income. In the existing literature, however, a continuous version of the Hicks model has not been considered yet. In consequence, little is known about its dynamic behavior.

The main purpose of this study is to shed light on this missing point and to demonstrate the following main results in a continuous Hicksian model: a birth of a limit cycle and the stabilizing effects of time delays. Following spirts of the original Hicks model, we take an upper bound for the output and a lower bound for the investment into account. These exogenous constraints imply that a resultant dynamic system is formed from four subsystems: in the first one neither constraints are effective, in the second one only upper constraint is effective, in the third one only the lower constraints is effective and in the fourth one both constraints are effective. Because of the switching of the subsystems during the adjustment process, it is technically difficult to consider the whole system analytically. In order to deal with this difficulty, we first construct a local stability/instability condition, next show the existence of a limit cycle in a 2D (i.e., two-dimensional) version of the model by applying the Poincarè-Bendixson

theorem and then numerically confirm that a 3D (i.e., three-dimensional) vesion can generate a limit cycle. It is also demonstrated that the consumption and/or the investment time lags have stabilizing effects in the both versions of the model.

The paper is organized as follows. In Section 2 a continuous version of a 2D Hicksian model is constructed with continuously distributed time delays in consumption and investment and its dynamics is considered. In Section 3, the 2D model is extended to a 3D model by introducing the further investment lag, and we perform simulations to find what dynamics the extended model can produce. Section 4 is for concluding remarks.

2 2D model

This section is divided into three parts. In Section 2.1, we introduce continuously distributed time lags and construct a continuous version of the Hicksian trade cycle model with floor and ceiling. In Section 2.2, the delay dynamic equation is transformed into a hybrid dynamic system of ordinary differential equations and then its local stability/instability conditions are considered. In Section 2.3, the global stability of the locally stable stationary point is numerically demonstrated and the existence of a piecewisely-connected limit cycle is analytically and numerically shown when the stationary state is locally unstable.

2.1 Hybrid model with continuously distributed time lag

The discrete version of a Hicksian trade cycle model is given by

$$\begin{aligned} C_t &= cY_{t-1}, \\ I_t &= \max[\beta(Y_{t-1} - Y_{t-2}), \ -I_L], \\ Y_t &= \min[C_t + I_t, \ Y^c]. \end{aligned} \tag{1}$$

Current consumption C_t is proportional to previous income Y_{t-1} where c is the marginal propensity to consumer, $0 < c < 1$. Investment I_t is proportional to the growth in the national income, as long as it is larger than the investment floor, $-I_L$. Income Y_t equals consumption plus investment, as long as it is smaller than the income ceiling, Y^c.

The three main features of the Hicksian model are the multiplier, the acceleration principle and the exogenous floor and ceiling. The first feature states that the current consumption is a fixed fraction of the delayed national income. The second shows that the investment is proportional to a fixed fraction of the delayed change in national income. The third prevents the decline of investment from depreciation and the increase of the output from the full-employment national income. Preserving these features, one possible continuous version of the Hicksian trade cycle model is constructed by the following three equations:

$$\begin{aligned} C(t) &= cY(t - \theta_c) \\ I(t) &= \max\left[\beta\dot{Y}(t - \theta_i), \ -I_L\right] \\ Y(t) &= \min\left[C(t) + I(t), \ Y^C\right] \end{aligned} \tag{2}$$

where θ_c is the consumption time lag and θ_i is the investment time lag. The similarity between (1) and (2) is clear. Since the lags are fixed in (2), this model is suitable for analyzing a situation in which the lengths of the time lags are certain. As pointed out by Hommes (1993,1995), Hicks presumes a more general situation in which both consumption and induced investment are distributed over several time periods. Taking account of this notion, a more appropriate version of the Hicksian trade cycle model with continuous time scales may be constructed by applying continuously distributed time delays:

$$\begin{aligned} C(t) &= cY_c^e(t), \\ I(t) &= \max\left[\beta \dot{Y}_i^e(t),\ -I_L\right], \\ Y(t) &= \min\left[C(t) + I(t),\ Y^C\right]. \end{aligned} \tag{3}$$

Here Y_c^e and $\dot{Y}_i^e$ are the expectations of the national income and the expected change of national income. It is assumed that these expectations are formed as weighted averages of the past realized values, respectively, in the following way:

$$Y_c^e(t) = \int_0^t \frac{1}{\theta_c} e^{-\frac{t-s}{\theta_c}} Y(s) ds$$

and

$$\dot{Y}_i^e(t) = \int_0^t \frac{1}{\theta_i} e^{-\frac{t-s}{\theta_i}} \dot{Y}(s) ds,$$

where θ_c and θ_i are positive constant which are considered as the proxies for the lengths of the time lags. The most weight is given to the most recent realized values and then the weight is exponentially declining. This particular form of the distribution function is often employed in order to simplify the dynamic analysis.[1] We call (3) the *basic distributed delay model*.

In the case of positive lags, differentiating the last two equations with respect to time gives the following 2D system of ordinary differential equations[2]:

$$\begin{cases} \dot{Y}_c^e(t) = \dfrac{1}{\theta_c}\left(Y(t) - Y_c^e(t)\right), \\ \ddot{Y}_i^e(t) = \dfrac{1}{\theta_i}\left(\dot{Y}(t) - \dot{Y}_i^e(t)\right), \end{cases} \tag{4}$$

It may be natural to assume that the investment lag is larger than or at least equal to the consumption lag:

Assumption 1. $\theta_c \leq \theta_i$.

[1] It is possible to replace the exponential kernel function with a general kernel function,

$$\frac{1}{n!}\left(\frac{n}{\theta}\right)^{n+1}(t-s)^n e^{-\frac{n(t-s)}{\theta}}$$

with finite n. However, this replacement may not change the qualitative aspects of the results to be obtained below.

[2] See the Appendix for constructing the same dynamical system in a different way.

Substituting the first and the second equations of (3) into the third one, we have the following output equation in the basic distributed delay model:

$$Y(t) = \min\left[cY_c^e(t) + \max\left[\beta\dot{Y}_i^e(t),\ -I_L\right],\ Y^C\right] \tag{5}$$

It turns out that the feasible $(Y_e^e, \dot{Y}_i^e)$-region is divided into four subregions by the following three partition lines,

$$\beta\dot{Y}_i^e(t) = -I_L,\ cY_c^e(t) + \beta\dot{Y}_i^e(t) = Y^C \text{ and } cY_c^e(t) - I_L = Y^C.$$

The four regions of the phase plane are defined as

$$R_A = \{(Y_c^e(t), \dot{Y}_i^e(t)) \mid \beta\dot{Y}_i^e(t) \geq -I_L \text{ and } cY_c^e(t) + \beta\dot{Y}_i^e(t) \leq Y^C\},$$

$$R_B = \{(Y_c^e(t), \dot{Y}_i^e(t)) \mid \beta\dot{Y}_i^e(t) \geq -I_L \text{ and } cY_c^e(t) + \beta\dot{Y}_i^e(t) > Y^C\},$$

$$R_C = \{(Y_c^e(t), \dot{Y}_i^e(t)) \mid \beta\dot{Y}_i^e(t) < -I_L \text{ and } cY_c^e(t) - I_L \leq Y^C\},$$

$$R_D = \{(Y_c^e(t), \dot{Y}_i^e(t)) \mid \beta\dot{Y}_i^e(t) < -I_L \text{ and } cY_c^e(t) - I_L > Y^C\}.$$

The negative-sloping partition line $cY_c^e + \beta\dot{Y}_i^e = Y^c$ distinguishes R_A from R_B, the horizontal partition line $\beta\dot{Y}_i^e = -I_L$ distinguishes R_A from R_C, and finally, the vertical partition line $cY_c^e - I_L = Y^c$ distinguishes R_C from R_D. Switches from one subregion to the another can occur only at points of the partition lines.

Before proceeding to the stability consideration of the delay hybrid system, we examine the stability of the system when there are no time lags, as a bench mark. To this end, we set $\theta_c = \theta_i = 0$ in (2) or $Y_c^e = Y$ and $\dot{Y}_i^e = \dot{Y}$ in (3) to derive the dynamic system without time lags:

$$Y(t) = \min[C(t) + \max[\beta\dot{Y}(t), -I_L], Y^c]$$

If $\beta\dot{Y}(t) > -I_L$ and $C(t) + \beta\dot{Y}(t) < Y^c$, we obtain a 1D differential equation,

$$\dot{Y}(t) = \frac{1-c}{\beta}Y(t).$$

It can be seen that $Y(t) = \dot{Y}(t) = 0$ is a stationary state, and applying the method of separation of variable gives the complete solution,

$$Y(t) = Y_0 e^{\lambda t} \text{ with } \lambda = \frac{1-c}{\beta} > 0.$$

Here Y_0 is an arbitrary initial point and λ is an eigenvalue. The positive eigenvalue implies instability of the stationary point. If $\beta\dot{Y}(t) \leq -I_L$, then, for all $t \geq 0$, we have

$$Y(t) = Y^c \text{ if } C(t) - I_L \geq Y^c \text{ or } Y(t) = -\frac{I_L}{1-c} \text{ if } C(t) - I_L < Y^c,$$

where Y^c is the maximum value (i.e., the ceiling) that $Y(t)$ can attain while $-I_L/(1-c)$ is the minimum (i.e., the floor). It is clear that although the stationary point is unstable, a trajectory does not diverge globally due to the ceiling and floor. In particular, if $Y_0 > 0$, then $Y(t)$ monotonically increases until it hits the ceiling and then stays there afterward. On the other hand, if $Y_0 < 0$, then $Y(t)$ monotonically decreases until it hits the floor and then stays there afterward. We summarize these results:

Theorem 1 *A continuous Hicksian model with no time lags is locally monotonically unstable, however, its output trajectory stays either at the ceiling or at the floor after it arrives there.*

2.2 Local stability

The national income is determined by (5). Since we have to distinguish between four regions, we analyze the stability/instability of system (4) under each of these four regions in this section while the over-all hybrid stability will be considered later in Section 2.3. For notational simplicity, let $x = Y_c^e$ and $y = \dot{Y}_i^e$. We next formulate the dynamic system in each region.

In R_A in which neither of the upper and lower bounds of (5) is effective, the national income and its rate of change are determined by

$$Y(t) = cx(t) + \beta y(t)$$

and

$$\dot{Y}(t) = c\dot{x}(t) + \beta\dot{y}(t).$$

Substituting these into (4) yields the linear dynamic system:

$$\begin{pmatrix} \dot{x}(t) \\ \\ \dot{y}(t) \end{pmatrix} = \begin{pmatrix} \dfrac{-(1-c)}{\theta_c} & \dfrac{\beta}{\theta_c} \\ \\ -\dfrac{c(1-c)}{(\theta_i-\beta)\theta_c} & -\dfrac{\theta_c - c\beta}{(\theta_i-\beta)\theta_c} \end{pmatrix} \begin{pmatrix} x(t) \\ \\ y(t) \end{pmatrix}. \tag{6}$$

It can be seen that the origin of the phase plane is the stationary state, which will be denoted by ε_A. Stability of (6) will be discussed later in this subsection.

In R_B the upper bound of national income is effective. The national income and its rate of change can be written as

$$Y(t) = Y^C$$

and

$$\dot{Y}(t) = 0.$$

Substituting these into (4) yields the relevant dynamic system for this region:

$$\begin{pmatrix} \dot{x}(t) \\ \\ \dot{y}(t) \end{pmatrix} = \begin{pmatrix} -\dfrac{1}{\theta_c} & 0 \\ \\ 0 & -\dfrac{1}{\theta_i} \end{pmatrix} \begin{pmatrix} x(t) \\ \\ y(t) \end{pmatrix} + \begin{pmatrix} \dfrac{Y^c}{\theta_c} \\ \\ 0 \end{pmatrix} \tag{7}$$

The stationary state is unique and denoted by $\varepsilon_B = (x_B, y_B)$ where $x_B = Y^C$ and $y_B = 0$. Since the eigenvalues of the coefficient matrix of system (7) are real and negative (i.e., $\lambda_1 = -\frac{1}{\theta_c}$ and $\lambda_2 = -\frac{1}{\theta_i}$), the stationary state is monotonically stable under R_B. Namely, any trajectory starting at a point inside of R_B approaches to the stationary state. The stationary state ε_B is, however, not located in R_B but in R_A, therefore, the trajectory soon or later crosses the partition line $cx + \beta y = Y^c$ and enters R_A in which the dynamic system switches to (6) from (7).

In R_C the lower bound of investment is effective, the national income and its rate of change are

$$Y(t) = cx(t) - I_L$$

and

$$\dot{Y}(t) = c\dot{x}(t).$$

Substituting these into (4) yields the following dynamic system:

$$\begin{pmatrix} \dot{x}(t) \\ \\ \dot{y}(t) \end{pmatrix} = \begin{pmatrix} -\dfrac{1-c}{\theta_c} & 0 \\ \\ -\dfrac{c(1-c)}{\theta_c\theta_i} & -\dfrac{1}{\theta_i} \end{pmatrix} \begin{pmatrix} x(t) \\ \\ y(t) \end{pmatrix} - \begin{pmatrix} \dfrac{I_L}{\theta_c} \\ \\ \dfrac{cI_L}{\theta_c\theta_i} \end{pmatrix} \tag{8}$$

The stationary state is unique and denoted by $\varepsilon_C = (x_C, y_C)$ with $x_C = -I_L/(1-c)$ and $y_C = 0$. Since the eigenvalues of the coefficient matrix of (8) are negative (i.e., $\lambda_1 = -\frac{1}{\theta_i}$ and $\lambda_2 = -\frac{1-c}{\theta_c}$), the stationary state of (8) is monotonically stable under R_C. Any trajectory starting at a point inside R_C is governed by system (8) as long as it stays within R_C. The stationary state is not located in R_C but in R_A. In consequence, the trajectory sooner or later crosses the partition line $\beta y = -I_L$ and enters R_A in which the dynamic system is switched to (6) from (8).

Finally, in R_D both of the upper and lower bounds are effective, the national income and its rate of change are determined by

$$Y(t) = Y^C$$

and

$$\dot{Y}(t) = 0.$$

Output determination in this region is the same as that in region R_B. As a result, the dynamic system in R_D is the same as the one defined in R_B and also the components of the stationary state are the same as those of system (7). In this sense, distinguishing R_D from R_B is expedient. Since R_D is adjacent to R_B and R_C and the stationary state of the dynamic system is in R_A, any trajectory starting within R_D will move into R_A through either R_B or R_C.

So far we have shown that all subsystems except (6) of the whole hybrid system are stable and the stationary states of these subsystems are located in R_A, the domain of the subsystem (6). Any trajectory starting at a point inside R_i for $i = B, C, D$ crosses one of the partitioning lines and enters R_A.

We now turn our attention to the stability of (6). The stability of ε_A depends on the eigenvalues of the coefficient matrix of (6),

$$J_A = \begin{pmatrix} -\dfrac{1-c}{\theta_c} & \dfrac{\beta}{\theta_c} \\ \\ -\dfrac{c(1-c)}{(\theta_i - \beta)\,\theta_c} & -\dfrac{\theta_c - c\beta}{(\theta_i - \beta)\,\theta_c} \end{pmatrix}.$$

The corresponding characteristic equation is

$$(\theta_i - \beta)\,\theta_c\lambda^2 + (\theta_c + (1-c)\theta_i - \beta)\,\lambda + (1-c) = 0.$$

The sum and product of the eigenvalues are given by

$$\lambda_1 + \lambda_2 = -\frac{\theta_c + (1-c)\theta_i - \beta}{(\theta_i - \beta)\,\theta_c}$$

and

$$\lambda_1 \lambda_2 = \frac{1-c}{(\theta_i - \beta)\,\theta_c}.$$

Since $0 < c < 1$, the stationary state is locally asymptotically stable if the parameters satisfy the following two conditions,

$$\theta_i - \beta > 0$$

and

$$\theta_c + (1-c)\theta_i - \beta > 0,$$

under which the real parts of the eigenvalues are negative.

In Figure 1, the stability region in the (θ_i, θ_c) space is shaded in light-gray and the instability region in dark-gray.[3] The ratio between the horizontal line and the vertical line is appropriately adjusted. Notice that the upward sloping line distinguishing the shaded regions from the white region is the diagonal line. In the white region above the diagonal line, Assumption 1 is violated. So any combination of (θ_i, θ_c) in the white region is eliminated from further considerations. Each of the shaded regions is further divided into two parts by the zero-discriminant curve of the characteristic equation defined by

$$\theta_c = (-1+2c)\beta + (1-c)\theta_i \pm 2\sqrt{(1-c)(\theta_i - \beta)c\beta}.$$

The stationary point ε_A is a focus for $(\theta_i,\ \theta_c)$ in the region inside the zero-discriminant curve and a node in the region outside. Roughly speaking, as observed in Figure 1, the stationary state is unstable under smaller values of the consumption and investment lags and becomes stable when either one or both of the lags becomes larger. In other words, introducing adequate lag sizes makes an otherwise unstable system stable. The stationary point of (6) is a unique stationary state of the whole system (4) whereas the stationary points ε_i for $i = B, C, D$ of the sub-dynamic systems are not stationary points of (4). The stability/instability of (6) is therefore equivalent to the local stability/instability of (4). In summary, we have the following result:

Theorem 2 *Given c and β, the basic distributed delay model is locally asymptotically stable in the light-gray region and locally unstable in the dark-gray region of the plane (θ_i, θ_c) shown in Figure 1 if an initial point is chosen in a neighborhood of the stationary point ε_A.*

[3] We refer to points denoted by S_A, S_B and U in Section 2.3.

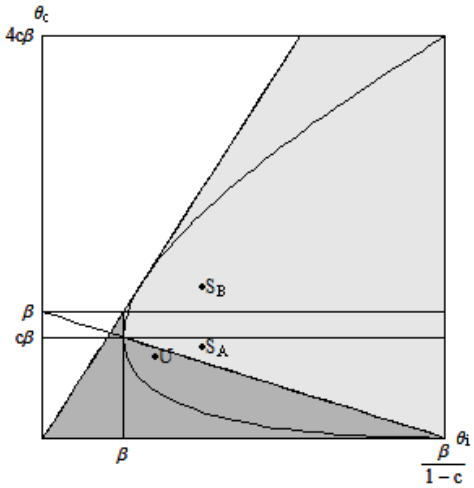

Figure 1. Partition of the stablity and instablity regions

It can be observed from Figure 1 that in the special case of $\theta_c = \theta_i = \theta$, the longer time lag can stabilize the system in the sense that the stationary state is unstable for $\theta < \beta$ and stable for $\theta > \beta$.

2.3 Global stability

So far, we have shown that the subsystems defined in R_B, R_C and R_D are locally stable if adjustments take place under the same regime throughout the entire process and that their stationary points ε_i^2 for $i = B, C, D$ are located in the inside of R_A. We have also shown in Theorem 1 that the local dynamic behavior of the whole system is the same as that of the subsystem (6), which depends on a combination of investment and consumption time lags, θ_i and θ_c. It remains to examine dynamic behavior in the large in which the system is subject to more than one regime during the adjustment process. It has not been mathematically proved yet that stability of all subsystems implies global stability of the whole hybrid continuous system.[4] We confirm the global stability when the stationary state is locally stable by performing numerical simulations and show the existence of a limit cycle when it is locally unstable by applying the Pointcarè-Bendixson theorem.

The dynamic system (4) is written, with newly introduced variables, x and y, by

$$\begin{cases} \dot{x}(t) = \dfrac{1}{\theta_c}\left(Y(t) - x(t)\right), \\ \\ \dot{y}(t) = \dfrac{1}{\theta_i}\left(\dot{Y}(t) - y(t)\right), \end{cases} \tag{9}$$

where $Y(t)$ and $\dot{Y}(t)$ take various forms, depending on the region in which a trajectory is located. The isoclines of $\dot{x}(t) = 0$ and $\dot{y}(t) = 0$ are central to a study of the motions of (9) in the (x, y) plane. It is derived from (7) and (8) that the isoclines in R_B and R_D are given by $x = Y^c$ and $y = 0$ while those

[4] Szidarovszky (2008) proves a sufficient condition for the global stability of piece-wise differentiable discrete dynamical systems.

in R_C by $x = I_L/c$ and $y = -(c(1-c)x + cI_L)/\theta_c$. From (6), the $\dot{x} = 0$ locus defined in R_A is given by

$$y = \frac{1-c}{\beta}x \tag{10}$$

which is positive-sloping and passes through the origin. Furthermore, it hits the partition line $cx + \beta y = Y^c$ at point $(Y^c, \frac{1-c}{\beta}Y^c)$ and the other partition line $\beta y = -I_L$ at point $(-\frac{1}{1-c}I_L, -\frac{1}{\beta}I_L)$. This $\dot{x} = 0$ locus is connected to the $\dot{x} = 0$ locus defined in R_B at the former point and to $\dot{x} = 0$ locus defined in R_C at the latter point. Clearly $\dot{x} > 0$ in the left of this constant locus and $\dot{x} < 0$ in the right. Provided that $\theta_c - c\beta \neq 0$, the $\dot{y} = 0$ locus defined in R_A is presented by

$$y = -\frac{c(1-c)}{\theta_c - c\beta}x. \tag{11}$$

Its slope depends on the value of the denominator: it is positive if $\theta_c < c\beta$ and negative if the inequality is reversed.[5] Furthermore, we assert that it becomes steeper than the partition line $cx + \beta y = Y^c$ if $c\beta < \theta_c < \beta$ and flatter if $\theta_c > \beta$. This $\dot{y} = 0$ locus is connected to the $\dot{y} = 0$ locus defined in R_C at a point on the partition line $\beta y = -I_L$. It is, however, not connected to the $\dot{y} = 0$ locus defined in R_B. Since the two isoclines, (10) and (11), are linear and intersect only once at the origin, the origin is the unique stationary point of the dynamic system. These isoclines are depicted as bold lines in Figure 2 in which the regions R_B and R_C are shaded in light-gray, R_D in dark-gray and the white region is R_A.

We now pursue global dynamic process when its stationary point is stable. We fix $\theta_i = 2.5$, $c = 0.8$, $\beta = 1.25$, $I_L = 10$ and $Y^c = 15$ throughout the numerical analysis of this section. Points S_A and S_B in Figure 1 correspond to $(2.5, 0.9)$ and $(2.5, 1.5)$, respectively, both of which are in the stable region. We first take point S_A for which (11) has a positive slope as $\theta_c < c\beta$. In Figure 2(left), the trajectories of (x, y) corresponding to 12 initial points of system (9) are depicted. We replace it with point S_B and the resultant simulations are depicted in Figure 2(right) in which the slope of (11) is negative and flatter than the slope of the $cx + \beta y = Y^c$ locus in absolute value as $\beta < \theta_c$. It is seen that the trajectories starting inside R_i for $i = B, C, D$ move into R_A. Although little is known about the global behavior when the dynamic system is piecewise linear, numerical simulations shown in Figures 2(left) and 2(right) reveal that regardless of the initial value of x and y, the trajectories are finally trapped inside region R_A and therefore converge to the stationary point. These numerical examples confirm the global stability of (9) when its stationary point is locally stable. This is summarized in

Simulation Result 1. *The basic distributed delay model is globally stable if its subsystem (6) is stable.*

[5] Needless to say (11) is not defined for $\theta_c = c\beta$. However the second equation of (6) implies that the $\dot{y} = 0$ locus is a vertical line passing through the origin when $\theta_c = c\beta$.

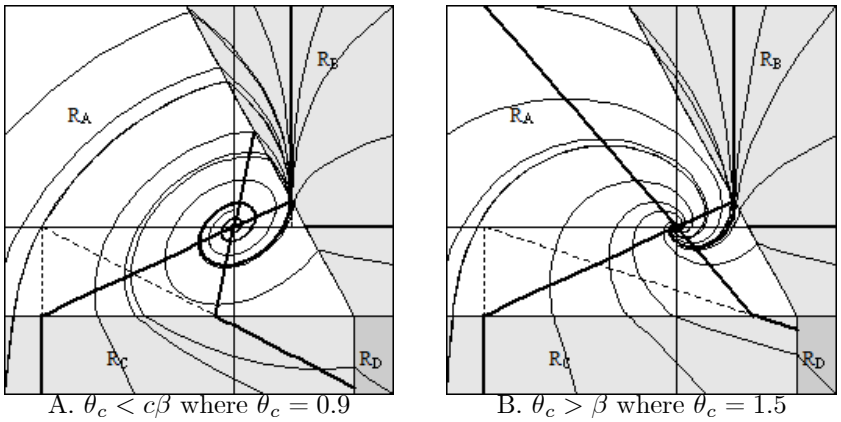

A. $\theta_c < c\beta$ where $\theta_c = 0.9$ B. $\theta_c > \beta$ where $\theta_c = 1.5$

Figure 2. Global stability when ε_A is locally stable

One remark should be made. We simulated the model many times with various combinations of the parameters' values and found that the Simulation Result 1 always holds. We incline to infer that the local stability of each subsystem leads to the global stability of the hybrid system. However, this is not proved mathematically yet.

We turn our attention to global dynamic behavior when the stationary state is locally unstable. To this end, we, first, construct an invariant region R in such a way that every trajectory starting outside the region enters it, and every trajectory starting inside it remains inside. Let the stationary point ε_C be point A and follow the forward trajectory of system (6) that rises out of the point A until it hits the partition line $\alpha x + \beta y = Y^C$ at point B. Let the intersection of the horizontal line starting at point B with the vertical line $x = Y^C$ be point C. The line segment CF is the $x = Y^C$ line and crosses the $\dot{x} = 0$ locus defined in R_A at point D, the horizontal $\beta y = -I_L$ line at point E and the $\dot{y} = 0$ locus defined in R_C at point F. We then draw the horizontal line starting at point F and ending at point G. The line segment connecting points G and A is the $(1-c)x = -I_L$ line that crosses the $\beta y = -I_L$ line at point H. Removing a small neighborhood of the stationary point from the region surrounded by the curve AB, the line segments, BC, CF FG and GA. The resultant region is R, which is bounded by the bold lines in Figure 3.

Next, we show that no trajectory leaves out of R. In particular, we ascertain that every trajectory beginning on the boundary of region R remains on the boundary or moves into the region. Let us considers, curve AB, line segments DE and HA in R_A. By (6), $\dot{x} < 0$ and $\dot{y} < 0$ on segment DE, $\dot{x} > 0$ and $\dot{y} > 0$ on segment HA and it is clear that any trajectory starting at a point on curve AB moves forward to point B on the curve. Let us then consider segments, BC and CD in R_B. By (7), $\dot{x} > 0$ and $\dot{y} < 0$ on segment BC while $\dot{x} = 0$ and $\dot{y} < 0$ on segment CD. Lastly consider segments, EF, FG and GH in R_C. By (8), $\dot{x} < 0$ and $\dot{y} < 0$ on segment EF where $\dot{y} = 0$ at point F, $\dot{x} < 0$ and $\dot{y} > 0$ on segment FG where $\dot{x} = 0$ at point G, and $\dot{x} > 0$ and $\dot{y} > 0$ on segment HA. Therefore any trajectory beginning on one of these segments must either stay there or moves inside the region R. It is also able to show that any trajectory beginning outside R must move into it within a finite time as shown by dotted

trajectories in Figure 3. Applying the Poincaré-Bendixon theorem reveals that there exists at least one limit cycle in the region R. The limit cycle is depicted as a bold curve within the region R and is bounded from above and below in Figure 3. We are now in a position to summarize the result obtained:

Theorem 3 *The basic distributed delay model gives rise to a constrained limit cycle if its subsystem (6) is unstable.*

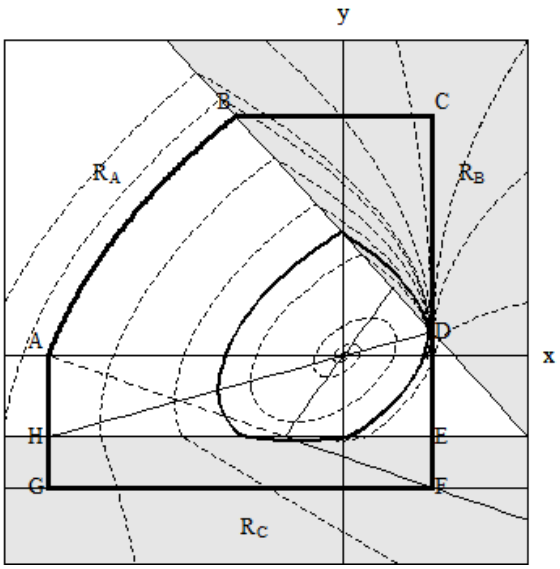

Figure 3. Construction of an inveraint region R

3 3D model

Hommes (1993, 1995) extends the discrete 2D Hicksian model (1) to a discrete 3D model in which consumption and investment are distributed over several periods and then shows that dynamic behavior of the system can become more complicated. We also extend the continuous 2D Hicksian model (4) to a continuous 3D model in which two different investment behavior are included: both investments have the accelerators related to the changes in past realized income, however, different investments have different weights to the changes. We construct a hybrid continuous 3D Hicksian model in Section 3.1, investigate stability of each subsystem in Section 3.2 and simulate the model to show the existence of a piecewisely-connected limit cycle in Section 3.3.

3.1 Hybrid model with two types of investment

The 3D continuous Hicksian model is given by the following equations:

$$\begin{aligned} C(t) &= cY_c^e(t) \\ I(t) &= \max\left[\beta_1\dot{Y}_1^e(t) + \beta_2\dot{Y}_2^e(t),\ -I_L\right] \\ Y(t) &= \min\left[C(t) + I(t),\ Y^C\right] \end{aligned} \tag{12}$$

where the expected consumption Y_c^e and the expected changes in national income $\dot{Y}_i^e$ for $i = 1, 2$ are defined as exponentially-weighted averages of the actual consumption and of the actual changes in national income in the past,

$$Y_c^e(t) = \int_0^t \frac{1}{\theta_c} e^{-\frac{t-s}{\theta_c}} Y(s) ds,$$

$$\dot{Y}_1^e(t) = \int_0^t \frac{1}{\theta_1} e^{-\frac{t-s}{\theta_1}} \dot{Y}(s) ds$$

and

$$\dot{Y}_2^e(t) = \int_0^t \frac{1}{\theta_2} e^{-\frac{t-s}{\theta_2}} \dot{Y}(s) ds.$$

Here, parameters β_1 and β_2 are the partial investment coefficients. The induced investment is, if not less than $-I_L$, the sum of proportions of the expected changes in national income, which have different distribution functions. Parameters θ_1 and θ_2 are proxies for the investment lags which are assumed not to be less than the proxy for the consumption lag:

Assumption 2. $\theta_c \leq \min[\theta_1, \theta_2]$

We call (12) the *extended distributed delay model*. Differentiating these expected variables with respect to time yields the following 3D dynamic system of ordinary differential equations,

$$\begin{cases} \dot{Y}_c^e(t) = \dfrac{1}{\theta_c} \left(Y(t) - Y_c^e(t) \right) \\ \ddot{Y}_1^e(t) = \dfrac{1}{\theta_1} \left(\dot{Y}(t) - \dot{Y}_1^e(t) \right) \\ \ddot{Y}_2^e(t) = \dfrac{1}{\theta_2} \left(\dot{Y}(t) - \dot{Y}_2^e(t) \right) \end{cases} \tag{13}$$

where

$$Y(t) = \min[cY_c^e(t) + I(t),\ Y^c]$$

and

$$I(t) = \max\left[\beta_1 \dot{Y}_1^e(t) + \beta_2 \dot{Y}_2^e(t),\ \ -I_L \right].$$

As in the case of the 2D system, the $(Y_c^e,\ \dot{Y}_1^e,\ \dot{Y}_2^e)$-space is divided into four regions by the following three partition planes:

$$\beta_1 \dot{Y}_1^e + \beta_2 \dot{Y}_2^e = -I_L,\ cY_c^e + \beta_1 \dot{Y}_1^e + \beta_2 \dot{Y}_2^e = Y^C \text{ and } cY_c^e = Y^C + I_L.$$

The four subregions are denoted by R_i^3 for $i = A, B, C, D$,

$$R_A^3 = \{(Y_e^e, \dot{Y}_1^e, \dot{Y}_2^e) \mid \textstyle\sum_{i=1}^2 \beta_i \dot{Y}_i^e(t) \geq -I_L \text{ and } cY_c^e(t) + \sum_{i=1}^2 \beta_i \dot{Y}_i^e(t) \leq Y^C\},$$

$$R_B^3 = \{(Y_e^e, \dot{Y}_1^e, \dot{Y}_2^e) \mid \textstyle\sum_{i=1}^2 \beta_i \dot{Y}_i^e(t) \geq -I_L \text{ and } cY_c^e(t) + \sum_{i=1}^2 \beta_i \dot{Y}_i^e(t) > Y^C\},$$

$$R_C^3 = \{(Y_e^e, \dot{Y}_1^e, \dot{Y}_2^e) \mid \textstyle\sum_{i=1}^2 \beta_i \dot{Y}_i^e(t) < -I_L \text{ and } cY_c^e(t) - I_L \leq Y^C\},$$

$$R_D^3 = \{(Y_e^e, \dot{Y}_1^e, \dot{Y}_2^e) \mid \textstyle\sum_{i=1}^2 \beta_i \dot{Y}_i^e(t) < -I_L \text{ and } cY_c^e(t) - I_L > Y^C\}.$$

For notational simplicity, let $x = Y_c^e$, $y = \dot{Y}_1^e$ and $z = \dot{Y}_2^e$. Then the dynamic system in each region is defined accordingly. If there are no time lags (that is, $Y_c^e = Y$, $\dot{Y}_1^e = \dot{Y}_2^e = \dot{Y}$), the output determination equation of (12) is reduced to (5) where β should be replaced with $\beta_1 + \beta_2$ and, therefore, the stationary state is locally unstable without time lags.

In R_A^3, $Y(t)$ and $\dot{Y}(t)$ are defined by

$$Y(t) = cx(t) + \beta_1 y(t) + \beta_2 z(t)$$

and

$$\dot{Y}(t) = c\dot{x}(t) + \beta_1 \dot{y}(t) + \beta_2 \dot{z}(t).$$

Substituting these relations into the dynamic equations (13) and rearranging terms give the corresponding dynamic system

$$\begin{cases} \dot{x}(t) = \dfrac{1}{\theta_c}\left(-(1-c)x(t) + \beta_1 y(t) + \beta_2 z(t)\right) \\ \dot{y}(t) = \dfrac{1}{\Delta}\left(-\dfrac{\theta_2(1-c)}{\theta_c}x(t) + \left(\dfrac{c\theta_2}{\theta_c}\beta_1 - (\theta_2 - \beta_2)\right) y(t) + \left(\dfrac{c\theta_2}{\theta_c} - 1\right)\beta_2 z(t)\right) \\ \dot{z}(t) = \dfrac{1}{\Delta}\left(-\dfrac{\theta_1(1-c)}{\theta_c}x(t) + \left(\dfrac{c\theta_1}{\theta_c} - 1\right)\beta_1 y(t) + \left(\dfrac{c\theta_1}{\theta_c}\beta_2 - (\theta_1 - \beta_1)\right) z(t)\right) \end{cases} \tag{14}$$

where $\Delta = (\beta_1 - \theta_1)(\beta_2 - \theta_2) - \beta_1\beta_2$. The stationary point is unique and denoted by $\varepsilon_A^3 = (x_A, y_A, z_A)$ with $x_A = 0$, $y_A = 0$ and $z_A = 0$. Stability of this system will be discussed rigorously in Section 3.2. In R_B^3, $Y(t)$ and $\dot{Y}(t)$ are defined by

$$Y(t) = Y^c$$

and

$$\dot{Y}(t) = 0.$$

Substituting these into the dynamic equations (13) gives the corresponding dynamic system:

$$\begin{cases} \dot{x}(t) = \dfrac{1}{\theta_c}\left(Y^c - x(t)\right), \\ \dot{y}(t) = \dfrac{1}{\theta_1}\left(-y(t)\right), \\ \dot{z}(t) = \dfrac{1}{\theta_2}\left(-z(t)\right). \end{cases} \tag{15}$$

The stationary point is unique and denoted by $\varepsilon_B^3 = (x_B, y_B, z_B)$ with $x_B = Y^c$, $y_B = z_B = 0$. It is stable as the eigenvalues of the associated Jacobian matrix are negative (i.e., $\lambda_1 = -\frac{1}{\theta_c}$, $\lambda_2 = -\frac{1}{\theta_1}$ and $\lambda_3 = -\frac{1}{\theta_2}$). The stationary point is, however, not located in R_B^3 but in R_A^3. A trajectory starting inside R_B^3 crosses the partition plane, $cx + \beta_1 y + \beta_2 z = Y^C$, and enters R_A^3 where the governing dynamic system is (14). In R_C^3, $Y(t)$ and $\dot{Y}(t)$ are defined by

$$Y(t) = cY_c^e(t) - I_L$$

and

$$\dot{Y}(t) = c\dot{Y}_c^e(t).$$

The corresponding dynamic system is

$$\begin{cases} \dot{x}(t) = \dfrac{1}{\theta_c}\left(-(1-c)x(t) - I_L\right), \\ \dot{y}(t) = \dfrac{1}{\theta_1}\left(-\dfrac{c(1-c)}{\theta_c}x(t) - y(t) - \dfrac{c}{\theta_c}I_L\right), \\ \dot{z}(t) = \dfrac{1}{\theta_2}\left(-\dfrac{c(1-c)}{\theta_c}x(t) - z(t) - \dfrac{c}{\theta_c}I_L\right). \end{cases} \tag{16}$$

The stationary point is unique and denoted by $\varepsilon_C^3 = (x_C, y_C, z_C)$ with $x_C = -\frac{1}{1-c}I_L$, $y_C = z_C = 0$. It is stable as the eigenvalues of the associated Jacobian matrix are negative (i.e., $\lambda_1 = -\frac{1-c}{\theta_c}$, $\lambda_2 = -\frac{1}{\theta_1}$ and $\lambda_3 = -\frac{1}{\theta_2}$). The stationary point is, however, not located in R_C^3 but in R_A^3. A trajectory starting inside R_C^3 crosses the partition plane, $\beta_1 y + \beta_2 z = -I_L$, and enters R_A^3 where the governing dynamic system is (14). In R_D^3, $Y(t)$ and $\dot{Y}(t)$ are defined by

$$Y(t) = Y^c$$

and

$$\dot{Y}(t) = 0.$$

The corresponding dynamic system is the same as (15) and its stationary state is equivalent to ε_B^3.

3.2 Local stability conditions

The stationary point ε_A^3 of the sub-system (14) is the inner point of R_A^3 and the unique stationary state of the whole system (13) while the stationary points ε_i^3 of the sub-dynamic systems for $i = B, C, D$ are not stationary points of (13). Our first job in this section is to find out whether or not the solution of (14) converges to the stationary state if an initial point is chosen in a neighborhood of the stationary point. The local stability is determined by the eigenvalues of the Jacobian matrix of (14), which has the form,

$$J = \begin{pmatrix} -\dfrac{1-c}{\theta_c} & \dfrac{\beta_1}{\theta_c} & \dfrac{\beta_2}{\theta_c} \\ -\dfrac{\theta_2 c(1-c)}{\Delta\theta_c} & \dfrac{1}{\Delta}\left(\dfrac{c\theta_2}{\theta_c} - (\theta_2 - \beta_2)\right) & \dfrac{1}{\Delta}\left(\dfrac{c\theta_2}{\theta_c} - 1\right)\beta_2 \\ -\dfrac{\theta_1 c(1-c)}{\Delta\theta_c} & \dfrac{1}{\Delta}\left(\dfrac{c\theta_1}{\theta_c} - 1\right)\beta_1 & \dfrac{1}{\Delta}\left(\dfrac{c\theta_1}{\theta_c} - (\theta_1 - \beta_1)\right) \end{pmatrix}.$$

The corresponding characteristic equation is

$$a_0\lambda^3 + a_1\lambda^2 + a_2\lambda + a_3 = 0$$

where the coefficients are given by

$$a_0 = \theta_c(\theta_1\theta_2 - \beta_1\theta_2 - \beta_2\theta_1),$$

$$a_1 = (1-c)\theta_1\theta_2 + (\theta_1+\theta_2)\theta_c - \beta_1(\theta_c+\theta_2) - \beta_2(\theta_c+\theta_1),$$

$$a_2 = (1-c)\theta_1 + (1-c)\theta_2 + \theta_c - \beta_1 - \beta_2,$$

$$a_3 = 1 - c > 0.$$

According to the Routh-Hurwitz stability criterion, the necessary and sufficient conditions that all roots of the characteristic equation have negative real parts are the following: all coefficients a_i for $i = 0, 1, 2$, are positive and $a_1a_2 - a_0a_3 > 0$.

We examine the shapes of the $a_i = 0$ curve for $i = 0, 1, 2$ and the $a_1a_2 - a_0a_3 = 0$ curve in the parameter region $\Theta = \{(\theta_1, \theta_2) \mid \theta_1 > 0 \text{ and } \theta_2 > 0\}$ and then look into the positional relationships among these curves to confirm the stability conditions.

We start with solving $a_0 = 0$ for θ_2 to obtain the following hyperbola,

$$\theta_2 = \frac{\beta_2\theta_1}{\theta_1 - \beta_1}, \tag{17}$$

which has a horizontal asymptote and a vertical asymptote, respectvely, at

$$\theta_2 = \beta_2 \text{ and } \theta_1 = \beta_1. \tag{18}$$

We assert that this hyperbola divides Θ into two parts: $a_0 > 0$ above the hyperbola and $a_0 < 0$ below. Next, solving $a_1 = 0$ for θ_2 yields also a hyperbola,

$$\theta_2 = \frac{(\theta_c - \beta_2)\theta_1 - (\beta_1 + \beta_2)\theta_c}{(\beta_1 - \theta_c) - (1-c)\theta_1}, \tag{19}$$

which has a horizontal asymptote and a vertical asymptote, respectively, at

$$\theta_2 = \frac{\beta_2 - \theta_c}{1-c} \text{ and } \theta_1 = \frac{\beta_1 - \theta_c}{1-c}. \tag{20}$$

We also assert that $a_1 > 0$ above the hyperbola (19) and $a_1 < 0$ below. Lastly, solving $a_2 = 0$ for θ_2 gives a negative sloping line,

$$\theta_2 = -\theta_1 + \frac{\beta_1 + \beta_2 - \theta_c}{1-c}, \tag{21}$$

where $a_2 > 0$ above this line and $a_2 < 0$ below.

To examine the positional relationship between the $a_0 = 0$ curve and the $a_1 = 0$ curve, we subtract the asymptotes of (20) from these of (18) to obtain

$$\beta_i - \frac{\beta_i - \theta_c}{1-c} = \frac{\theta_c - c\beta_i}{1-c} \text{ for } i = 1, 2.$$

The following five cases are identified depending on the signs of $\theta_c - c\beta_i$ for $i = 1, 2$:

Result (1). *If* $\theta_c < c\min[\beta_1, \beta_2]$ *holds, then the* $a_0 = 0$ *curve is below the* $a_1 = 0$ *curve.*

Result (2). *If* $c\beta_1 < \theta_c < c\beta_2$ *holds, then the* $a_0 = 0$ *curve intersects the* $a_1 = 0$ *curve from above to below at point* (θ_1^L, θ_2^L) *where*

$$\theta_1^L = \frac{-\beta_1\theta_c + \sqrt{\beta_1\beta_1\left(c\left(\beta_1+\beta_2\right)-\theta_c\right)\theta_c}}{c\beta_2 - \theta_c}$$

and

$$\theta_2^L = \frac{-\beta_2\theta_c - \sqrt{\beta_1\beta_1\left(c\left(\beta_1+\beta_2\right)-\theta_c\right)\theta_c}}{c\beta_1 - \theta_c}.$$

Result (3). *If* $c\beta_2 < \theta_c < c\beta_1$ *holds, then the* $a_0 = 0$ *curve intersects the* $a_1 = 0$ *curve from left to right at point* $(\theta_1^\ell, \theta_2^\ell)$ *where*

$$\theta_1^\ell = \frac{-\beta_1\theta_c - \sqrt{\beta_1\beta_1\left(c\left(\beta_1+\beta_2\right)-\theta_c\right)\theta_c}}{c\beta_2 - \theta_c}$$

and

$$\theta_2^\ell = \frac{-\beta_2\theta_c + \sqrt{\beta_1\beta_1\left(c\left(\beta_1+\beta_2\right)-\theta_c\right)\theta_c}}{c\beta_1 - \theta_c}.$$

Result (4a). *If* $\max[c\beta_1, c\beta_2] < \theta_c$ *and* $\theta_c < c(\beta_1+\beta_2)$ *hold, then the* $a_0 = 0$ *curve intersects the* $a_1 = 0$ *curve twice at* (θ_1^L, θ_2^L) *and* $(\theta_1^\ell, \theta_2^\ell)$.

Result (4b). *If* $\max[c\beta_1, c\beta_2] < \theta_c$ *and* $c(\beta_1+\beta_2) < \theta_c$ *hold, then the* $a_0 = 0$ *curve is above the* $a_1 = 0$ *curve.*

To examine the positional relationship between the $a_0 = 0$ curve and the $a_2 = 0$ curve, we equate (21) to (17) and solve the resultant equation for θ_1 to have

$$\theta_1^\pm = \frac{(2-c)\beta_1 + c\beta_2 - \theta_c \pm \sqrt{d_{02}}}{2(1-c)} \tag{22}$$

where the discriminant d_{02} is given by

$$d_{02} = \left(\theta_c - c\left(\beta_1+\beta_2\right)\right)^2 - 4\beta_1\beta_2(1-c)^2. \tag{23}$$

The two curves intersect if the discriminant is positive and do not if negative. The threshold values of θ_c to make the discrimiant zero is obtained by solving $d_{02} = 0$,

$$\theta_c^\pm = c(\beta_1+\beta_2) \pm 2(1-c)\sqrt{\beta_1\beta_2}. \tag{24}$$

Then we have the following results;

Result (5). *The* $a_0 = 0$ *curve intersects the* $a_2 = 0$ *curve twice if* $\theta_c < \theta_c^-$ *or* $\theta_c^+ > \theta_c$ *and is located aove the* $a_2 = 0$ *curve otherwise.*

Lastly, to examine the positional relationship between the $a_1 = 0$ curve and the $a_2 = 0$ curve, we equate (19) to (21) and solve the resultant equation for θ_1 to have

$$\theta_{1\pm} = \frac{(2-c)\beta_1 + c\beta_2 - \theta_c \pm \sqrt{d_{12}}}{2(1-c)}$$

where the discriminant d_{12} is given by

$$d_{12} = -3\theta_c^2 + 4c(\beta_1 + \beta_2)\theta_c - 4\beta_1\beta_2. \tag{25}$$

The two curves intersect if the discriminant is positive and do not if negative. The threshold values of θ_c to make the discrimiant zero is obtained by solving $d_{12} = 0$,

$$\theta_{c\pm} = \frac{2}{3}\left(c(\beta_1 + \beta_2) \pm \sqrt{c^2(\beta_1 + \beta_2)^2 - 3\beta_1\beta_2}\right).$$

Then we have the following results;

Result (6). *The $a_1 = 0$ curve intersects the $a_2 = 0$ curve twice if $c > \frac{\sqrt{3\beta_1\beta_2}}{\beta_1+\beta 2}$ and is above the $a_2 = 0$ curve otherwise.*

We turn to confirm a shape of the $a_1a_2 - a_0a_3 = 0$ curve. To this end, simplifying assumptions are made: $\beta_1 < \beta_2$ and c is given in such a way to satisfy

$$c(\sqrt{\beta_1} + \sqrt{\beta_2})^2 < 4\sqrt{\beta_1\beta_2} \text{ or } c < \frac{4\sqrt{\beta_1\beta_2}}{(\sqrt{\beta_1} + \sqrt{\beta_2})^2}. \tag{26}$$

Then we have the following results, the proof of which is given in the Appendix B.

Result (7). *The following three cases are identified in the appropriate region of θ_1 and θ_2:*

(7-1) *If $\theta_c < \theta_c^A$, then the $a_1a_2 - a_0a_3 = 0$ curve is decribed by two downward-sloping curves*:

(7-2) *If $\theta_c^A < \theta_c < \theta_c^B$, then it is decsribed by a half-closed and half-opened curve*:

(7-3) *If $\theta_c^B < \theta_c$, then it is described by a closed curve where*

$$\theta_c^A = \left(\frac{\sqrt{c}\left(\sqrt{\beta_1} - \sqrt{\beta_2}\right) + \sqrt{c\left(\sqrt{\beta_1} - \sqrt{\beta_2}\right)^2 + 4\sqrt{\beta_1\beta_2}}}{2}\right)^2$$

and

$$\theta_c^B = \left(\frac{\sqrt{c}\left(\sqrt{\beta_2} - \sqrt{\beta_1}\right) + \sqrt{c\left(\sqrt{\beta_1} - \sqrt{\beta_2}\right)^2 + 4\sqrt{\beta_1\beta_2}}}{2}\right)^2.$$

Two remarkes are given. The first is that $\theta_c^A > \theta_c^B$ holds if $\beta_1 > \beta_2$ is assumed. It then follows that θ_c^A and θ_c^B in (7-1), (7-2) and (7-3) should be replaced each other. The second is that in the special case of $\beta_1 = \beta_2 = \beta$, $\theta_c^A = \theta_c^B = \beta$ holds and thus (7-2) should be eliminated: the $a_1a_2 - a_0a_3 = 0$ curve is decribed by two downward-sloping curves if $\theta_c < \beta$ and by a closed curve if $\theta_c > \beta$.

We verify Result (7) numerically. We fix $c = 0.8$ throughout the numerical analysis below and illustrate the different shapes of the curve in Figure 4, changing values of β_1, β_2 and θ_c. We take $\theta_c = 0.5$ and $\beta_1 = \beta_2 = 0.6$, which satisfy the condition, $\theta_c < \beta$. The loci of θ_1 and θ_2 for which $a_1a_2 - a_0a_3 = 0$ holds are depicted as two downward-sloping curves in Figure 4(left). They divide the region Θ into three parts. $a_1a_2 - a_0a_3 > 0$ holds in the shaded regions and the inequality is reversed in the white region. In Figure 4(right), $\beta_1 = \beta_2 = 0.6$ is preserved, however, $\theta_c = 0.5$ is replaced with $\theta_c = 0.65$, which fulfills the condition $\beta < \theta_c$. As a result, the $a_1a_2 - a_0a_3 = 0$ curve becomes a closed curve and divides region Θ into two segments: the inside and outside parts of the closed curve. Light gray and white colors of the divided regions have the same meanings as those in Figure 4(left). In these two examples, $\beta_1 = \beta_2$ is taken only for simplicity. Qualitatively similar curves can be obtained even if $\beta_1 \neq \beta_2$. However, when $\beta_1 \neq \beta_2$, the third case emerges in which θ_c is larger than β_i but less than β_j. The $a_1a_2 - a_0a_3 = 0$ curve becomes a half-closed and half-open curve. In particular, the upper parts of the two curves are joined together and the lower parts are still disconnected as depicted in Figure 4(middle) in which $\theta_c = 0.65$, $\beta_1 = 0.6$ and $\beta_2 = 0.7$ are taken to satisfy $\theta_c^A < \theta_c < \theta_c^B$. On the other hand, the lower parts become connected and the upper parts remain disconnected if $\beta_1 > \beta_2$ and $\theta_c^B < \theta_c < \theta_c^A$, although this case is not illustrated in Figure 4.

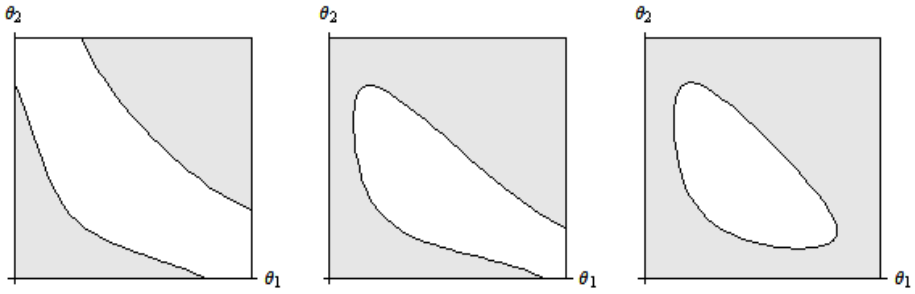

Figure 4. Various shapes of the $a_1a_2 - a_0a_3 = 0$ curve

3.3 Global stability

We now determine the stability/instability region of Θ and simulate the model under different values of the model's parameters to find out what kind of dynamics the hybrid system (13) can generate. Before proceeding, we make the following assumptions for the sake of analytical simplifity.

Assumption 3. $\dfrac{2\sqrt{\beta_1\beta 2}}{(\sqrt{\beta_1}+\sqrt{\beta_2})^2} < c < \dfrac{\sqrt{3\beta_1\beta 2}}{\beta_1+\beta_2}$.

Four remarkes regarding Assumption 3 are given. First, the maximum values of $\frac{2\sqrt{\beta_1\beta 2}}{(\sqrt{\beta_1}+\sqrt{\beta_2})^2}$ and $\frac{\sqrt{3\beta_1\beta 2}}{\beta_1+\beta_2}$ that are attained for $\beta_1 = \beta_2$ are $\frac{1}{2}$ and $\frac{\sqrt{3}}{2}$. It would be natural to assume the marignal propensity consume c is larger than the former but less than the latter.[6] Second, the first inequality of Assumption 3 imply that the smaller threshold value, θ_c^-, given in (24) are positive. Third, Result (6) and the second inequality imply that the $a_1 = 0$ curve is always above the $a_2 = 0$ curve. Lastly, the second inequality also implies that the inequlity in (26) always holds.

We first examine the case in which $c = 0.8$, $\theta_c = 0.35$ and $\beta_1 = \beta_2 = 0.6$ are taken. Under these parameter specifications, $c\beta_1 = c\beta_2 = 0.48$, $\theta_c^A = \theta_c^B = 0.6$, $\theta_c^- = 0.72$ and $\theta_c^+ = 1.2$. In consequence, we have $\theta_c < \min[c\beta_1, c\beta_2]$. Result (1) implies that the $a_0 = 0$ curve is below the $a_1 = 0$ curve. We also have $\theta_c < \theta_c^- < \theta_c^+$ that leads to the positive d_{02}. Result (6) and Assumption 3 imply that the $a_1 = 0$ curve does not intersect the $a_2 = 0$ curve. Lastly, we have $\theta_c < \theta_c^A$. Result (7-1) implies that the $a_1a_2 - a_0a_3 = 0$ curve is described by the two downward sloping bold curves. All curves are depicted in Figure 5(left). The real hyperbolas and the dotted hyperbolas corresponds to the $a_0 = 0$ curve and the $a_1 = 0$ curve, respectively. The $a_2 = 0$ curve is the negative-sloping dashed line. Points A and B are the intersections of the last two curves. By (21) and (22), they are $(3.52, 0.72)$ and $(0.72, 3.52)$. The two bold curves are the $a_1a_2 - a_0a_3 = 0$ curve. It is seen that the lower $a_1a_2 - a_0a_3 = 0$ curve passes through points A and B because $a_0 = a_2 = 0$ imply $a_1a_2 - a_0a_3 = 0$.

Notice that $a_1a_2 - a_0a_3 = -a_0a_3 < 0$ on the $a_1 = 0$ curve. Hence the upper $a_1a_2 - a_0a_3 = 0$ curve is located above it. The Routh-Hurwitz stability conditions are fulfilled above this $a_1a_2 - a_0a_3 = 0$ curve. Therefore the upper $a_1a_2 - a_0a_3 = 0$ curve is the boundary between the stability region and the instability region. In Figure 5(left), the stable region of Θ is shaded in light-gray color, the region in which Assumption 2 is violated in dark-gray and the remaining white region is the unstable region.

A simulation is performed by taking $\theta_1 = 3$, $\theta_2 = 2.5$, $x(0) = 0.1$, $y(0) = 0.1$ and $z(0) = 0$. The birth of a limit cycle is seen in Figure 5(right). The black dot in Figure 5(left) denotes the selected point $(3, 2.5)$ of the investment time lags. Since the dot is in the white region, the stationary point is locally unstable. The trajectory starting in the neighborhood of the stationary point moves away from the stationary point.[7] The dynamic system (13) is the hybrid system in which the subsystems switch when the trajectory hits either of the ceiling or floor and moves one regime to another during the adjustment process. The parts of the floor and the ceiling are depicted as the shaded planes. It can be observed that by these restrictions the trajectory is prevented from diverging and converges

[6] The violation of the second inequality does not harm the results to be obtained below, however, makes the analysis complicated.

[7] It depends on the value of the discriminant of the cubic characteristic equation whether the trajectory explodes monotonically or oscillatory. The discrimiant is given by

$$(a_1a_2)^2 - 4a_1^3a_3 - 4a_0a_2^3 + 18a_0a_1a_2a_3 - 27(a_0a_3)^2.$$

To decrease the complexity of further dividing Θ, the loci of θ_1 and θ_2 for which this dicriminant is zero is not depicted in the following figures.

to a limit cycle.

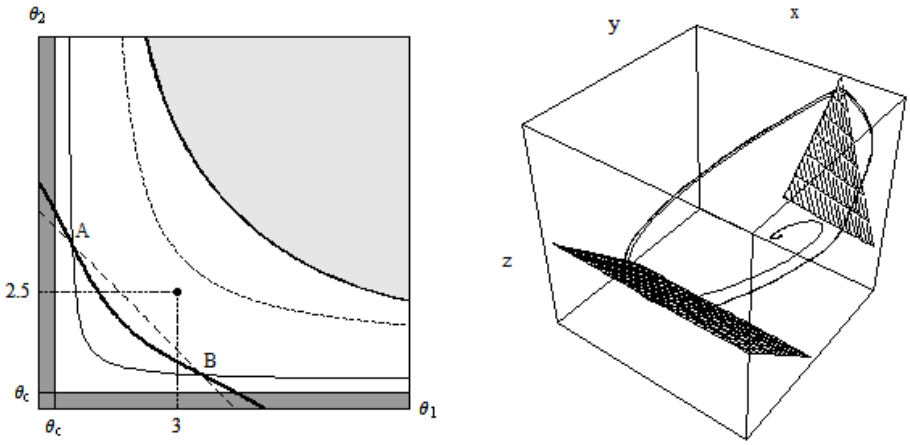

Figure 5. $\theta_c < c\min[\beta_1, \beta_2]$

In the second example we deal with the case in which $\theta_c = 0.65$, $\beta_1 = 0.6$, and $\beta_2 = 0.85$. Since $c\beta_1 = 0.48$, $c\beta_2 = 0.68$, we have $c\beta_1 < \theta_c < c\beta_2$. Result (2) implies that the $a_0 = 0$ curve intersects the $a_1 = 0$ curve from above at $(\theta_1^L, \theta_2^L) = (0.71, 4.71)$ which is denoted as point C in Figure 6(left). $\theta_c^A = 0.611$ and $\theta_c^B = 0.835$ leads to $\theta_c^A < \theta_c < \theta_c^B$, with which Result (7-2) implies that the $a_1a_2 - a_0a_3 = 0$ curve is a half-closed and half-opend curve. Further, from (24), we have $\theta_c^- = 0.875$ and $\theta_c^+ = 1.446$ that leads to $\theta_c < \theta_c^- < \theta_c^+$. Result (5) implies that the $a_0 = 0$ curve intersect the a_2 curve twice. These intersections are denoted as point $A = (0.82, 3.18)$ and point $B = (2.93, 1.07)$ in Figure 6(left). Under these parameter values, the division of Θ is presented in Figure 6(left). For simulations, we choose the black dot in Figure 6(left) that corresponds to the point of $\theta_1 = 3.5$ and $\theta_2 = 2.5$. Since the dot is in the white region, the stationary point is unstable. However it can be observed in Figure 6(right) that the hybrid system (13) gives rise to a limit cycle which is bounded from above and below.

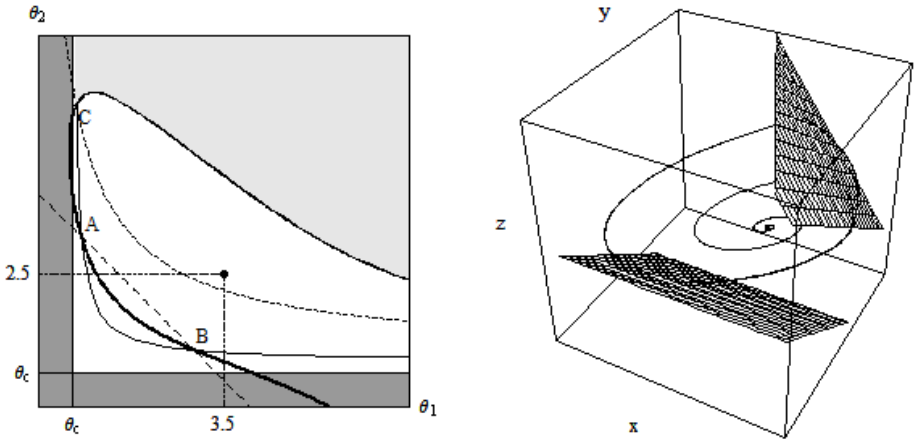

Figure 6. $c\beta_1 < \theta_c < c\beta_2$ and $\beta_1 < \theta_c < \beta_2$

In the third and final example, we take $\theta_c = 0.65$, $\beta_1 = 0.6$ and $\beta_2 = 0.6$ which generate $c\beta_1 = c\beta_2 = 0.6$, $\theta_c^A = \theta_c^B = 0.6$, $\theta_c^- = 0.72$ and $\theta_c^+ = 1.2$. We then have $c\max(\beta_1, \beta_1) < \theta_c$, $\theta_c < c(\beta_1 + \beta_2)$, $\theta_c^B < \theta_c$ and $\theta_c < \theta_c^-$. Thus, Result (4a), Result (5) and Result (7-3) imply that the $a_0 = 0$ curve intersects, twice, not only the $a_1 = 0$ curve at point $C = (0.71, 3.88)$ and point $D = (3.88, 0.71)$ but also the $a_2 = 0$ curve at point $A = (0.88, 1.87)$ and point $B = (1.87, 0.88)$. They also imply that the $a_1a_2 - a_0a_3 = 0$ curve becomes a closed curve. Since $a_0 = a_2 = 0$ at points A and B and $a_0 = a_1 = 0$ at point C and D, the $a_1a_2 - a_0a_3 = 0$ curve passes through these points as depicted in Figure 7 (left). The divided regions of Θ have the same meanings as those of Figure 5 and 6 if the color is the same. Since the dot in Figure 7(left) is the point of the selected $\theta_1 = 3$ and $\theta_2 = 2.5$ and is in the white region, the stationary point is locally unstable. A numerical simulation in Figure 7(right) shows that a limit cycle is born and bounded from above and below.

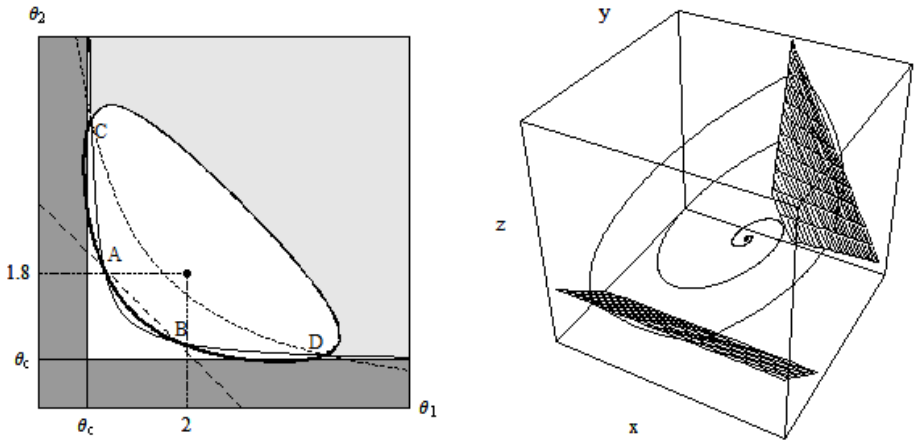

Figure 7. $\max[c\beta_1, c\beta_2] < \theta_c$ and $\theta_c < c(\beta_1 + \beta_2)$

We summarize these simulation results:

Simulation Result 2 *The extended distributed delay model gives rise to a constrained limit cycle if (14) is unstable.*

We simulate the model with even higher value of θ_c that satisfies $c(\beta_1+\beta_2) < \theta_c$ and obtain qualitatively the same results. As can be seen in the right panels of Figures 5, 6 and 7, the dark-shaded region becomes larger by making some parts of the stable and unstable regions infeasible as θ_c increases. For some higher values of θ_c, it is possible that the white region is absorbed by the dark-gray regions and the dynamic system becomes stable for all θ_1 and θ_2 that fulfill Assumption 2.

4 Concluding Remarks

We have considered the dynamics of a continuous Hicksian business cycle model with floor and ceiling. It is shown first, as a bench mark, that the model without time delays is always locally unstable. Introducing continuously distributed time

delays in consumption and investment, the following two main results are then demonstrated: (1) larger delays in consumption and/or investment stabilize the stationary state; (2) an upper and/or lower bounded limit cycle is developed when the stationary state is unstable.

Appendix A

As has been shown, differentiating $Y_c^e(t)$ with respect to t yields the differential equation,

$$\dot{Y}_c^e(t) = \frac{1}{\theta_c}\left(Y(t) - Y_c^e(t)\right). \tag{A-1}$$

Applying integration by parts for the right hand side of $\dot{Y}_i^e(t)$, we have

$$\dot{Y}_i^e(t) = \frac{1}{\theta_i}Y(t) - \frac{1}{\theta_i}Y(0)e^{-\frac{t}{\theta_i}} - \frac{1}{\theta_i}\int_0^t \frac{1}{\theta_i}e^{-\frac{t-s}{\theta_i}}Y(s)ds.$$

If we denote the last integral by $Y_i^E(t)$, differentiating it with respect to time yields the differential equation

$$\dot{Y}_i^E(t) = \frac{1}{\theta_i}\left(Y(t) - Y_c^E(t)\right) \tag{A-2}$$

and

$$\dot{Y}_i^e(t) = \frac{1}{\theta_i}Y(t) - \frac{1}{\theta_i}e^{-\frac{t}{\theta_i}}Y(0) - \frac{1}{\theta_i}Y_i^E(t). \tag{A-3}$$

In order to see the similarity between this system and the original system (4), we confine our attention to the region R_A^2 in which $Y(t) = cY_c^e(t) + \beta\dot{Y}_i^e(t)$. Substituting (A-3) into the right hand side of $Y(t) = cY_c^e(t) + \beta\dot{Y}_i^e(t)$ and solving the resultant equation for $Y(t)$ imply that

$$Y(t) = \frac{c\theta_i}{\theta_i - \beta}Y_c^e(t) - \frac{\beta}{\theta_i - \beta}Y_i^E(t) - \frac{\beta}{\theta_i - \beta}Y(0)e^{-\frac{t}{\theta_i}}.$$

This is further substituted into (A-1) and (A-2) to obtain the dynamic equation in terms of Y_i^e and Y_i^E:

$$\begin{pmatrix} \dot{Y}_c^e(t) \\ \\ \dot{Y}_i^E(t) \end{pmatrix} = \begin{pmatrix} \frac{\beta-(1-c)\theta_i}{\theta_c(\theta_i-\beta)} & -\frac{\beta}{\theta_c(\theta_i-\beta)} \\ \\ \frac{c}{\theta_i-\beta} & -\frac{1}{\theta_i-\beta} \end{pmatrix} \begin{pmatrix} Y_i^e(t) \\ \\ Y_i^E(t) \end{pmatrix} - \begin{pmatrix} \frac{\beta}{\theta_c(\theta_i-\beta)}Y(0)e^{-\frac{t}{\theta_i}} \\ \\ \frac{\beta}{\theta_c(\theta_i-\beta)}Y(0)e^{-\frac{t}{\theta_i}} \end{pmatrix}.$$

The characteristic equation of the Jacobian matrix of this system is identical with that of (6). This means that this dynamic system generates the same dynamics in a neighborhood of the equilibrium point as the original dynamic system. Furthermore, if we choose the initial points of both system in such a way that

$$\dot{Y}_i^e(0) = -\frac{1}{\theta_i}Y_i^E(0),$$

then they generate identical dynamics.

Appendix B

This appendix proves Result (7). Collecting together terms of $a_1a_2 - a_0a_3$ involving the same powers of objects matching θ_2 yields

$$a_1a_2 - a_0a_3 = A\theta_2^2 + B\theta_2 + C$$

where the coefficients A, B and C are given by

$$A = -(1-c)\left(\beta_1 - \theta_c - (1-c)\theta_1\right),$$

$$B = \left(\beta_1 + \beta_2 - (1-c)\theta_1 - \theta_c\right)^2 - \beta_2\left(\beta_1 + \beta_2 + c\theta_c\right)$$

and

$$C = \left(\beta_1 + \beta_2 - \theta_1\right)\beta_1\theta_c + \left(\beta_1 + \beta_2 - \theta_c\right)\left(\theta_1 + \theta_2\right) - \left(\beta_2\theta_1 + \left(\beta_1 - \theta_1\right)\theta_c\right)\left((1-c)\theta_1 + \theta_c\right).$$

Solving $A\theta_2^2 + B\theta_2 + C = 0$ for θ_2 yields two functions of θ_1

$$\varphi_1(\theta_1) = \frac{-B + \sqrt{B^2 - 4AC}}{2A} \text{ and } \varphi_2(\theta_1) = \frac{-B - \sqrt{B^2 - 4AC}}{2A}.$$

The discriminant $B^2 - 4AC$ is a fourth-order equation of θ_1. Solving $B^2 - 4AC = 0$ for θ_1 gives the following four roots,

$$\theta_1^1 = \frac{\beta_1 - \sqrt{c\beta_1\theta_c} - \sqrt{\left(\sqrt{\theta_c} - \sqrt{c\beta_1}\right)^2\theta_c - \left(\sqrt{c\theta_c} - \sqrt{\beta_1}\right)^2\beta_2}}{1-c},$$

$$\theta_1^2 = \frac{\beta_1 - \sqrt{c\beta_1\theta_c} + \sqrt{\left(\sqrt{\theta_c} - \sqrt{c\beta_1}\right)^2\theta_c - \left(\sqrt{c\theta_c} - \sqrt{\beta_1}\right)^2\beta_2}}{1-c},$$

$$\theta_1^3 = \frac{\beta_1 + \sqrt{c\beta_1\theta_c} - \sqrt{\left(\sqrt{\theta_c} + \sqrt{c\beta_1}\right)^2\theta_c - \left(\sqrt{c\theta_c} + \sqrt{\beta_1}\right)^2\beta_2}}{1-c}$$

and

$$\theta_1^4 = \frac{\beta_1 + \sqrt{c\beta_1\theta_c} + \sqrt{\left(\sqrt{\theta_c} + \sqrt{c\beta_1}\right)^2\theta_c - \left(\sqrt{c\theta_c} + \sqrt{\beta_1}\right)^2\beta_2}}{1-c}.$$

Let us denote the discriminants of the first two equations and the last two equations, respectively, as

$$f(\theta_c) = \left(\sqrt{\theta_c} - \sqrt{c\beta_1}\right)^2\theta_c - \left(\sqrt{c\theta_c} - \sqrt{\beta_1}\right)^2\beta_2$$

and

$$g(\theta_c) = \left(\sqrt{\theta_c} + \sqrt{c\beta_1}\right)^2\theta_c - \left(\sqrt{c\theta_c} + \sqrt{\beta_1}\right)^2\beta_2.$$

$f(\theta_c)$ can be factored as

$$\left(\theta_c - \sqrt{c}\left(\sqrt{\beta_1} - \sqrt{\beta_2}\right)\sqrt{\theta_c} - \sqrt{\beta_1\beta_2}\right)\left(\theta_c - \sqrt{c}\left(\sqrt{\beta_1} + \sqrt{\beta_2}\right)\sqrt{\theta_c} + \sqrt{\beta_1\beta_2}\right).$$

Since the first factor and the second factor are quadratic in$\sqrt{\theta_c}$, the threshold values of $\sqrt{\theta_c}$ that make $f(\theta_c)$ equal to zero are obtained by solving $f(\theta_c) = 0$,

$$\sqrt{\theta_c^{1,2}} = \frac{\sqrt{c}\left(\sqrt{\beta_1} - \sqrt{\beta_2}\right) \pm \sqrt{c\left(\sqrt{\beta_1} - \sqrt{\beta_2}\right)^2 + 4\sqrt{\beta_1\beta_2}}}{2}.$$

and

$$\sqrt{\theta_c^{3,4}} = \frac{\sqrt{c}\left(\sqrt{\beta_1} - \sqrt{\beta_2}\right) \pm \sqrt{c\left(\sqrt{\beta_1} - \sqrt{\beta_2}\right)^2 - 4\sqrt{\beta_1\beta_2}}}{2}.$$

In the similar way, $g(\theta_c)$ can be factored as

$$\left(\theta_c + \sqrt{c}\left(\sqrt{\beta_1} + \sqrt{\beta_2}\right)\sqrt{\theta_c} + \sqrt{\beta_1\beta_2}\right)\left(\theta_c - \sqrt{c}\left(\sqrt{\beta_1} + \sqrt{\beta_2}\right)\sqrt{\theta_c} - \sqrt{\beta_1\beta_2}\right)$$

where the first factor is always positive. The threshold values of $\sqrt{\theta_c}$ that make $g(\theta_c)$ equal to zero are obtained by solving $g(\theta_c) = 0$,

$$\sqrt{\theta_c^{5,6}} = \frac{\sqrt{c}\left(\sqrt{\beta_2} - \sqrt{\beta_1}\right) \pm \sqrt{c\left(\sqrt{\beta_2} - \sqrt{\beta_1}\right)^2 + 4\sqrt{\beta_1\beta_2}}}{2}.$$

Since $c\left(\sqrt{\beta_1} - \sqrt{\beta_2}\right)^2 - 4\sqrt{\beta_1\beta_2} < 0$ holds under Assumption 3, $\sqrt{\theta_c^{3,4}}$ are complex conjugates. It can be found that the smaller roots of $\sqrt{\theta_c^{1,2}}$ and $\sqrt{\theta_c^{5,6}}$ are real and negative, which does not make sense. Let us denote the larger roots by θ_c^A and θ_c^B that are rewritten as

$$\theta_c^A = \left(\frac{\sqrt{c}\left(\sqrt{\beta_1} - \sqrt{\beta_2}\right) + \sqrt{c\left(\sqrt{\beta_1} - \sqrt{\beta_2}\right)^2 + 4\sqrt{\beta_1\beta_2}}}{2}\right)^2$$

and

$$\theta_c^B = \left(\frac{\sqrt{c}\left(\sqrt{\beta_2} - \sqrt{\beta_1}\right) + \sqrt{c\left(\sqrt{\beta_2} - \sqrt{\beta_1}\right)^2 + 4\sqrt{\beta_1\beta_2}}}{2}\right)^2$$

The assumption $\beta_1 < \beta_2$ leads to $\theta_c^A < \theta_c^B$. If $0 < \theta_c < \theta_c^A$, then $g(\theta_c) < f(\theta_c) < 0$, which implies that θ_1^i for $i = 1, 2, 3, 4$ are complex. Hence $\varphi_1(\theta_1)$ and $\varphi_2(\theta_1)$ take different values for any θ_1 except $\bar{\theta}_1 = (\beta_1 - \theta_c)/(1 - c)$. This proves (7-1). If $\theta_c^A < \theta_c < \theta_c^B$, then $g(\theta_c) < 0 < f(\theta_c)$, which implies that θ_1^i for $i = 1, 2$ are real and θ_1^i for $i = 3, 4$ are complex. Hence, $\varphi_1(\theta_1^i) = \varphi_2(\theta_1^i)$ for $i = 1, 2$, which means that both curves are connected at each of these two points. As numerically shown below, θ_1^1 is small enough to be less than θ_c or becomes negative, depending on θ_c. It is eliminated from the appropriated region of Θ. This proves (7-2). Lastly if $\theta_c^B < \theta_c$, then $0 < g(\theta_c) < f(\theta_c)$, which implies that θ_1^i is real and hence $\varphi_1(\theta_1^i) = \varphi_2(\theta_1^i)$ for $i = 1, 2, 3, 4$. Both curves are connected at each of these four points. As is also numerically shown below, since θ_1^1 is small enough to be less than θ_c or becomes negative while θ_1^4 is extremely large or $\varphi_1(\theta_1^4) = \varphi_2(\theta_1^4)$ becomes negative. these two points are also eliminated from the appropriate region of Θ. This proves (7-3).

Taking $c = 0.8$, $\beta_1 = 0.7$ and $\beta_2 = 0.75$, we numerically confirm (7-2) and (7-3). First, we have $\theta_c^A \simeq 0.702$ and $\theta_c^B \simeq 0.747$. Suppose $\theta_c = 0.72$, which satisfies

$\theta_c^A < \theta_c < \theta_c^B$. Then we have the connecting points, $(\theta_1^1, \varphi_i(\theta_1^1)) \simeq (0.07, 10.7)$ and $(\theta_1^2, \varphi_i(\theta_1^2)) \simeq (0.59, 5.1)$ for $i = 1, 2$. In Figure A(left), the real curve is the $\theta_2 = \varphi_1(\theta_1)$ locus and the dotted curve is the $\theta_2 = \varphi_2(\theta_1)$ locus. Two curves are seen to be connected at the point $(\theta_1^2, \varphi_i(\theta_1^2))$. Next suppose $\theta_c = 0.76$, which satisfies $\theta_c^B < \theta_c$. The four connecting points are $(\theta_1^1, \varphi_i(\theta_1^1)) \simeq (-0.24, 18.2)$, $(\theta_1^2, \varphi_i(\theta_1^2)) \simeq (0.72, 4.09)$, $(\theta_1^3, \varphi_i(\theta_1^3)) \simeq (5.82, 0.828)$ and $(\theta_1^4, \varphi_i(\theta_1^4)) \simeq (7.70, -0.14)$. Two curves are connected at the second and third points and constructs a closed curve in Figure A(right) in which the first point and the fourth points are eliminated.

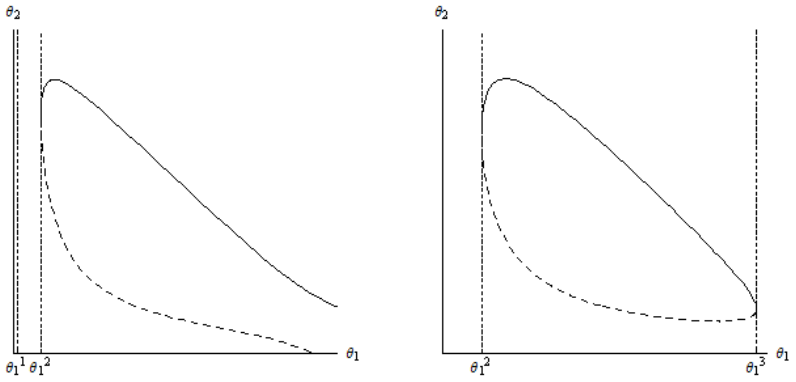

Figure A. $a_1 a_2 - a_0 a_3 = 0$ curves

References

Chang, W. W. and D. J. Smyth, "The Existence and Persistence of Cycles in a Non-Linear Model: Kaldor's 1940 Model Re-examined," *Review of Economic Studies*, 38, 37-44, 1971.

Dana, R. A. and P. Malgrange, "The Dynamics of a Discrete Version of a Growth Cycle Model," in *Analyzing the Structural Economic Models*, ed.., J. P. Ancot, The Hague: Martinus Nijhoff, 205-222, 1984.

Gardini, L., T. Puu and I. Sushko, "The Hicksian Model with Investment Floor and Income Ceiling," in *Business Cycle Dynamics: Models and Tools*, ed. by T. Puu and I. Sushko, Berlin/NewYork: Springer-Verlag, 179-191, 2006.

Goodwin, R., "The nonlinear accelerator and the persistence of business cycles," *Econometrica*, 1-17,1951.

Hicks, J. R. *A contribution to the theory of the trade cycle*, Clarendon Press, Oxford, 1950.

Hommes, C., "Periodic, almost periodic and chaotic behavior in Hicks' nonlinear trade cycle model," *Economic Letters,* 41, 391-397, 1993.

Hommes, C., "A reconsideration of Hicks' non-linear trade cycle model," *Structural Changes and Economic Dynamics,* 6, 435-459, 1995.

Kaldor, N., "A model of the trade cycle," *Economic Journal*, 50, 78-92, 1940.

Lorenz, H-W., "Goodwin's Nonlinear Accelerator and Chaotic Motion," *Journal of Economics*, 47, 413-418, 1987.

Lorenz, H-W., *Nonlinear Dynamical Economics and Chaotic Motion*, 2nd edition, Berlin/NewYork/Tokyo, Springer-Verlag, 1993.

Matsumoto, A., "Note on Goodwin's 1951 Nonlinear Accelerator Model wit an Investment Lag," mimeo (submitted), 2008.

Puu, T., "The Hicksian Trade Cycle with Floor and Ceiling Dependent on Capital Stock," *Journal of Economic Dynamics and Control*, 31, 575-592, 2007.

Sushko, I., T. Puu and L. Gardini, "A Goodwin-Type Model with Cubic Investment Function,"in *Business Cycle Dynamics: Models and Tools*, ed. by T. Puu and I. Sushko, Berlin/NewYork: Springer-Verlag, 299-316, 2006.

Szidarovszky, F., "Some Notes on the Asymptotical Stability of Dynamic Economic Systems," mimeo, 2008.